JACS
JOURNAL OF THE AMERICAN CHEMICAL SOCIETY

COMMUNICATION

pubs.acs.org/JACS

# Thermally Controlled Cyclic Insertion/Ejection of Dopant Ions and Reversible Zinc Blende/Wurtzite Phase Changes in ZnS Nanostructures

Niladri S. Karan,[†] Suresh Sarkar,[§,†] D. D. Sarma,[‡] Paromita Kundu,[⊥] N. Ravishankar,[⊥] and Narayan Pradhan*[,§,†]

[§]Department of Materials Science and [†]Centre for Advanced Materials, Indian Association for the Cultivation of Science, Jadavpur, Kolkata 700032, India

[‡]Solid State and Structural Chemistry Unit, and [⊥]Materials Research Centre, Indian Institute of Science, Bangalore 560012, India

Supporting Information

**ABSTRACT:** We report a reversible phase transformation of platelet-shaped ZnS nanostructures between wurtzite (WZ) and zinc blende (ZB) phases by reversible insertion/ejection of dopant Mn(II) ions induced by a thermocyclic process. In a reaction flask loaded with WZ ZnS platelets and Mn molecular precursors, during heating Mn ions are incorporated and change the phase of the host nanostructures to ZB; during cooling Mn ions are spontaneously ejected, returning the host nanoplatelets to the original WZ phase. These reversible changes are monitored for several cycles with PL, EPR, XRD, and HRTEM. Interestingly, the (0001) WZ platelets transform to (110) ZB following a nucleation and growth process triggered by a local increase/depletion of the $Mn^{2+}$ concentration in the nanocrystals.

While material properties depend invariably on phase and composition, nanocrystals (NCs) are in a size domain where the properties are also sensitive functions of the material size and shape.[1] Early developments in nanoscience and nanotechnology focused primarily on controlling the shape and size, particularly for semiconductor NCs,[1,2] to bring about previously unimaginable tunability of materials properties, opening up new paths to technological innovations and applications.[3] After control of the size and shape of NCs was mastered, the focus shifted to tuning the composition[4] (often via doping[5]) and crystalline phase[6] of nanomaterials, as these are known to alter material properties significantly, even in the macroscopic size regime. Formation of semiconductor NCs with deterministic control over size, shape, phase, and composition is critical for realizing many multifunctional nanodevice applications.[3] While there has been considerable progress in changing these parameters in various NCs systems, almost all such changes have been irreversible. For example, one may start with semiconductor NCs doped with a transition metal ion and place them in an environment (e.g. at elevated temperature) that induces expulsion of dopant ions, but there is no easy procedure to incorporate the expelled dopant ions back into the NCs.[7]

Similarly, by controlling the synthesis or reaction conditions, phase changes in semiconductor NCs have been achieved irreversibly by the application of temperature,[8] deformation,[9] high-energy radiation,[10] by introduction of dopants,[11] or by variation of the stabilizing ligands.[12] This suggests that, for all reaction conditions explored so far, there is a sizable energy difference between the two states of NCs involved, e.g. between the doped and undoped states or the two crystallographic phases of the same NCs, precluding the possibility of cycling at will between the two states of a given NC with significantly different properties and functionalities.[13]

**Scheme 1. Temperature-Induced Dopant Insertion/Ejection and Phase Change of 2D ZnS Nanoplatelets**

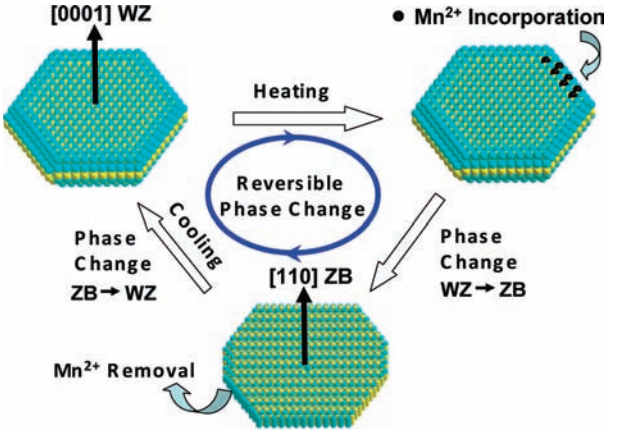


Here we report a reversible crystal phase transition of two-dimensional (2D) ZnS nanostructures (platelets or disks) in colloidal solution from an as-synthesized wurtzite (WZ) phase to a cubic zinc blende (ZB) structure, controlled by a concomitant, reversible inclusion/exclusion of $Mn^{2+}$ ions from a precursor (Scheme 1), establishing for the first time that it is possible to realize a near equilibrium between two different states of a NC system. Making use of sharply contrasting properties of these two phases, we prove with photoluminescence (PL) and electron paramagnetic resonance (EPR) that the change to cubic phase is initiated by doping of $Mn^{2+}$ in platelet-shaped NCs at $T > 180$ °C, while the ejection of $Mn^{2+}$ from the NC at $T < 180$ °C leads to transformation back to the WZ phase, with the transformation being reversible for as many cycles as we tested. Interestingly, the (0001) WZ platelets transform to (110) ZB following a phase nucleation and growth process triggered by a local increase/depletion of $Mn^{2+}$ concentration in the NC. Our approach opens up a new way to engineer the composition and phase in anisotropic semiconductor NCs and is expected to strengthen

**Received:** October 26, 2010
**Published:** January 25, 2011





dx.doi.org/10.1021/ja109625v | J. Am. Chem. Soc. 2011, 133, 1666–1669

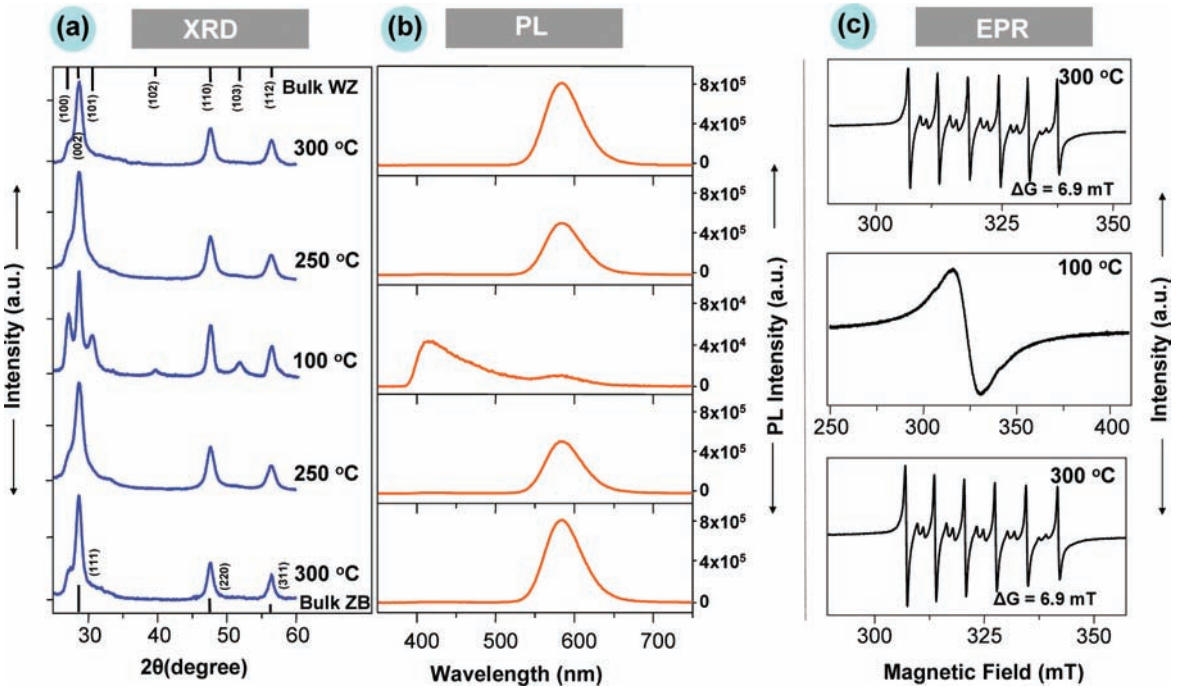


**Figure 1.** (a) XRD and (b) PL spectra of samples collected at different temperatures during a thermal cycling process, 300−100−300 °C, of a particular reaction system. Bulk XRD peaks for ZB and WZ ZnS are provided for comparison. The emission centered at ∼585 nm corresponds to Mn dopant emission. Excitation wavelength, 320 nm. (c) EPR of samples collected from the same reaction system at 300 °C (bottom), during cooling to 100 °C (middle), and after reheating to 300 °C (top).

the understanding of fundamental aspects of adsorption of dopants in semiconductor hosts and possible dopant-induced reversible shape and phase conversions.

Platelet-shaped ZnS (∼14 nm wide, ∼1.2 nm height) nanodisks are chosen here for dopant-induced reversible phase change. Hexagonal-shaped WZ ZnS platelets are synthesized by a high-temperature injection colloidal synthetic method. In a typical process, zinc diethyldithiocarbamate dissolved in oleylamine is injected into hot hexadecylamine (HDA) at 300 °C and then annealed at 280 °C for 5 min, resulting in WZ ZnS nanoplatelets. For the phase change of these nanoplatelets, the reaction mixture is then cooled to 100 °C, 0.8% (molar, compared to Zn) of manganese diethyldithiocarbamate in oleylamine is injected, and the reaction temperature is gradually increased again to 300 °C (details in Supporting Information (SI)). It has been observed that during heating and cooling of the reaction mixture, the PL spectra as well as the crystal phase of the ZnS change reversibly. However, the high-temperature phase can be retained by quenching the reaction mixture to room temperature by injecting it into cold acetone for flocculation.

Figure 1a shows room temperature X-ray diffraction (XRD) patterns of ZnS samples after $Mn^{2+}$ incorporation into the reaction system for one complete temperature cycle (300 → 100 → 300 °C). To obtain diffraction patterns, these samples were collected from the reaction mixture and quenched from temperatures indicated in the figure as specified above. XRD patterns of ZB and WZ bulk ZnS are also shown in the figure for comparison. The change of the crystallographic phase of ZnS successively from the cubic ZB at 300 and 250 °C to the hexagonal WZ at 100 °C and back to the ZB on increasing the temperature again is clearly evident from the appearance and disappearance of characteristic diffraction peaks (Figure 1a) of respective crystal structures. This reversible change in the crystallographic phase of ZnS nanoplatelets is accompanied by an equally spectacular and reversible change in the PL behavior of these samples on temperature cycling. PL spectra of the aliquots at different temperatures are shown in Figure 1b for the same temperature cycle as in Figure 1a. The topmost panel in Figure 1b, corresponding to the sample quenched from 300 °C, shows a reasonably intense (quantum efficiency ∼10%) PL peak at ∼585 nm, typical of a $Mn^{2+}$ $^4T_1$—$^6A_1$ transition in Mn-doped ZnS and related nanoparticles.[5a,5j,14] Samples quenched from 250 °C exhibit the same PL emission from doped Mn with somewhat lower intensity. A drastic change is noticed in the PL spectrum for the sample at 100 °C. Emission from doped $Mn^{2+}$ ions becomes very weak, along with the appearance of a new emission feature at 400−500 nm, which is clearly dominated by surface trap emission of undoped ZnS nanomaterials.[14c] The absence of dopant emission in samples obtained at lower temperature (<180 °C) with WZ structure strongly suggests very effective ejection of doped $Mn^{2+}$ ions from the WZ lattice in these samples. Increasing the temperature of the reaction mixture back to 250 or 300 °C regenerates the $Mn^{2+}$-related emission, along with the disappearance of the trap-state emission, indicating ZnS nanoplatelets are once again doped with Mn. The close correspondence between the reversible changes in the crystallographic phases and in the emission properties (equivalently doping/undoping of Mn into the lattice) suggests that these two aspects are closely connected in a cause-and-effect relationship. We have observed the phase change and the appearance/disappearance of dopant and surface emissions for several cycles reproducibly. It is important to note that the phase change is not observed in the absence of $Mn^{2+}$ dopant ions, and the WZ phase of ZnS nanoparticles is observed throughout the temperature cycle for the undoped case (SI, Figure S1). Clearly, the reversible phase change is critically dependent on the presence of dopant ions and temperature cycling.


dx.doi.org/10.1021/ja109625v |*J. Am. Chem. Soc.* 2011, 133, 1666–1669

The presence of dopant $Mn^{2+}$ ions in the lattice of ZnS nanoplatelets formed at 300 °C is established by EPR spectra (Figure 1c). For the ZB sample quenched from 300 °C, six characteristic hyperfine splittings of isolated $Mn^{2+}$ ions are observed with a hyperfine splitting constant of 6.9 mT, suggesting dopant $Mn^{2+}$ ions at the tetrahedral lattice sites of ZnS nanostructures.[5a,7c,15] This hyperfine splitting disappears for ZnS samples collected below 180 °C; instead, a broad signal appears most of the time, probably due to clustered or concentrated $Mn^{2+}$ions on the surface of ZnS platelets. We found no EPR signal when the sample collected below 180 °C was washed thoroughly, supporting the notion that $Mn^{2+}$ ions are completely ejected from the NC lattice below 180 °C. This change in the EPR spectrum from six hyperfine splittings characteristic of isolated $Mn^{2+}$ ions doped in the lattice to a broad or no signal, indicating an absence of $Mn^{2+}$ ions in the lattice, is also found to be reversible, mirroring the change in the crystallographic phase and the PL emission, with systematic variation in the reaction temperature. Moreover, this suggests the whole process follows the transformation of ZnS and MnS to Mn-doped ZnS in the hot reaction system.

To obtain direct microscopic evidence and an understanding of the mechanism of the crystallographic phase change on temperature cycling in the present case, we carried out detailed studies using high-resolution transmission electron microscopy (HRTEM) on samples obtained by quenching the reaction mixture from different temperatures. Figure 2a,b shows HRTEM images of thoroughly washed WZ nanoplatelets collected at 100 °C and ZB nanoplatelets collected at 300 °C. From the HRTEM images, the lattice spacing is found to be 3.3 Å (Figure 2c), corresponding to $\{11\bar{2}0\}$ planes of WZ ZnS viewed along the [0001] axis, for samples collected at $T <$ 180 °C; lattice spacings of 3.1 and 2.7 Å (Figure 2d), corresponding to the {111} and {002} planes of ZB ZnS along the [110] axis, respectively, are seen for samples collected at $T >$180 °C. Several TEM images of both WZ and ZB platelets are also shown in the SI (Figures S2 and S3). In contrast to the present case, transformation between WZ and ZB phases generally takes place such that the [0001] axis of WZ is parallel to the [111] axis of ZB.[13a,16] Mechanistically, this is easily explained in terms of the introduction of periodic stacking faults connecting the ABCA arrangement of the ZB structure to the ABAB arrangement of the WZ structure. However, in this case, the [0001]-oriented platelets of WZ ZnS change to their ZB counterparts with a [110] orientation rather than the expected [111] orientation. This indicates that the transformation does *not* proceed by the introduction of stacking faults in the parent structure. The fact that the high-temperature ZB phase could be retained at room temperature by quenching suggests that the transformation between the two phases is diffusional in nature. From all these observations, we can now propose a mechanism for the uniquely reversible changes observed on temperature cycling of the reaction mixture. We believe that Mn diffusion into the ZnS nanoplatelets, naturally enhanced with increasing temperature, leads to nucleation of the cubic phase within the WZ platelets; subsequent growth of these nucleated ZB sites completely converts the platelets to the ZB phase. This interpretation is supported by our TEM images of samples obtained around 180 °C, where we both crystallographic phases in a single nanoplatelet of ZnS, as shown in the HRTEM image in Figure 2e. On increasing the temperature beyond 180 °C, the ZB phase is seen forming at the periphery of the platelet. The FFT pattern taken from this image shows spacings corresponding to the (002) plane of the ZB phase. The origin of the nucleation of the ZB phase invariably at the edge of the WZ nanoplatelets indicates that the

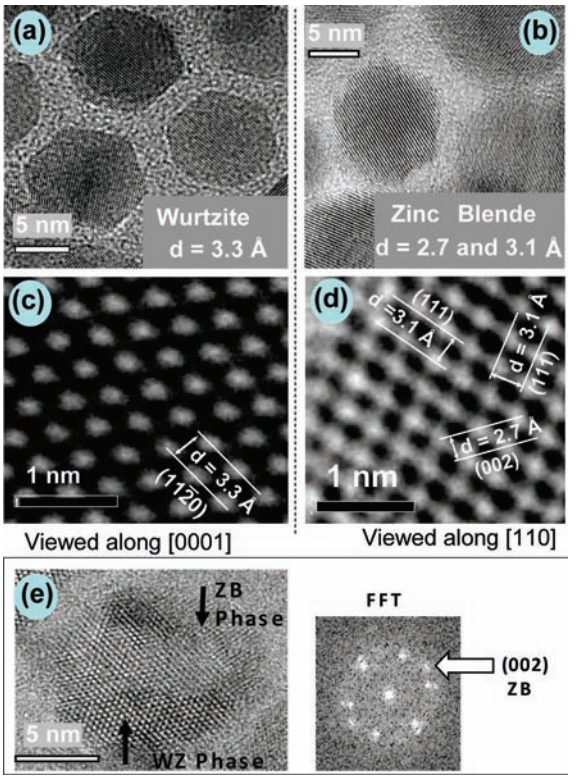


**Figure 2.** HRTEM images of (a) WZ and (b) ZB ZnS platelets; (c,d) the corresponding magnified HRTEM images. (e) An intermediate TEM image showing the existence of both WZ and ZB phases in a single platelet. Right, the FFT with identification of the (002) plane of ZB ZnS.

edge provides convenient sites for Mn adsorption in this case, understandable in view of the fact that edge atoms have the least coordination and, therefore, are more reactive toward all species in general. Additionally, within the WZ platelets, the 110 facet of the ZB phase has the lowest surface energy,[17] making it the preferred orientation for the face of the nanoplatelet in the ZB phase.

Above, we have discussed the mechanism of transformation between the two phases in terms of diffusion of Mn, nucleation of the Mn-doped ZB phase of ZnS, and its growth controlled by atomic diffusion rather than by the generation of stacking faults involving relative motions of entire atomic planes. Our observations suggest that the WZ phase without any Mn is the lowest energy state for $T <$ 180 °C, while the Mn-containing ZB phase is stable above 180 °C, with the two phases being nearly degenerate at $T \approx$ 180 °C. The reason for this is difficult to establish due to the complexity of the problem. However, it appears clear that in addition to the presence of $Mn^{2+}$ ions as dopant, subtle changes in interaction strengths of the specific capping agent, namely oleylamine/HDA, with different faces of ZB and WZ nanoplatelets are crucial in determining the relative stability of these two phases. This is made evident by our observation that ligands such as thiols or carboxylic acids that bind strongly arrest the transformation process, stabilizing the system in the crystallographic form independent of temperature. Thus, it is essential to have labile binding of amine ligands on the surface of the nanoplatelets whose adsorption at lower temperatures and desorption at higher temperatures change the energy stability between ZB and WZ phases gently. However, this is not in itself sufficient to bring about the near degeneracy between the two

phases discussed above. The transformation between these two phases is assisted by nucleation and growth of Mn-dopant-stabilized ZB phase at higher temperatures, as indicated by Figure 2e. This is further supported by the observation that this transformation of WZ platelets to the ZB phase at any given temperature proceeds over a period of time (Figure S4, SI); the rate of change of the crystal phase increases with increasing temperature. This suggests that there is a certain induction time associated with the phase change, which is reduced at higher temperatures, as expected for a nucleation and growth mechanism. During this phase change, most of the hexagonal-shaped nanoplatelets transform to nearly circular or irregular hexagonal platelets and vice versa (Figures S2 and S3, SI).

In conclusion, we report a dopant-induced reversible phase change of 2D ZnS nanoplatelets in a colloidal solution. Incorporation of $Mn^{2+}$ into ZnS nanoplatelets in the WZ phase at and above ~180 °C nucleates the ZB phase, which then grows, converting the entire platelet to the ZB form. During the cooling cycle, these Mn-doped ZB platelets return to the WZ structure, ejecting the doped Mn ions from the lattice. This reversible crystallographic phase change is accompanied by corresponding drastic changes in PL properties and EPR spectra, in addition to obvious changes in XRD patterns. While normal phase transformation between WZ and ZB structures would be expected to convert the planar arrangements along the [0001] axis of WZ to the [111] of ZB, in this case we observed a change from [0001] of WZ to [110] of ZB, suggesting individual atomic rearrangements. These results provide a contrasting example of (reversible) expulsion of dopant ions at lower temperatures, compared to examples of (irreversible) expulsion of dopant ions at higher temperatures, referred to as "self-purification" in the past literature. We have observed this temperature cycling induced reversible dopant insertion/ejection and reversible phase change for these 2D nanoplatelets of ZnS nanostructures and not for spherical ZnS nanocrystals. We are at present investing the possibility of such changes with different shapes as well as in other NC systems.

## ■ ASSOCIATED CONTENT

**Supporting Information.** Details of the materials, methods, supporting figures. This material is available free of charge via the Internet at http://pubs.acs.org.

## ■ AUTHOR INFORMATION

**Corresponding Author**
camnp@iacs.res.in

## ■ ACKNOWLEDGMENT

Department of Science and Technology, India, is acknowledged for funding. N.S.K. acknowledges CSIR, India. J. C. Bose (D.D.S.) and LNJ Bhilwara (N.P.) are acknowledged for fellowships.

## ■ REFERENCES

(1) (a) Murray, C. B.; Norris, D. J.; Bawendi, M. G. *J. Am. Chem. Soc.* **1993**, *115*, 8706–8715. (b) Manna, L.; Scher, E. C.; Alivisatos, A. P. *J. Am. Chem. Soc.* **2000**, *122*, 12700–12706. (c) Peng, Z. A.; Peng, X. *J. Am. Chem. Soc.* **2001**, *123*, 183–184. (d) Hu, J.; Li, L.; Yang, W.; Manna, L.; Wang, L.; Alivisatos, A. P. *Science* **2001**, *292*, 2060–2063. (e) Talapin, D. V.; Rogach, A. L.; Kornowski, A.; Haase, M.; Weller, H. *Nano Lett.* **2001**, *1*, 207–211. (f) Manna, L.; Milliron, D. J.; Meisel, A.; Scher, E. C.; Alivisatos, A. P. *Nat. Mater.* **2003**, *2*, 382–385. (g) Schmid, G. *Chem. Rev.* **1992**, *92*, 1709–1727. (h) Brust, M.; Bethell, D.; Schiffrin, D. J.; Kiely, C. J. *Adv. Mater.* **1995**, *7*, 795–797. (i) Zheng, J.; Zhang, C.; Dickson, R. M. *Phys. Rev. Lett.* **2004**, *93*, 077402/1–077402/4.

(2) (a) Peng, X.; Manna, U.; Yang, W.; Wickham, J.; Scher, E.; Kadavanich, A.; Alivisatos, A. P. *Nature* **2000**, *404*, 59–61. (b) Peng, Z. A.; Peng, X. *J. Am. Chem. Soc.* **2002**, *124*, 3343–3353. (c) Joo, J.; Na, H. B.; Yu, T.; Yu, J. H.; Kim, Y. W.; Wu, F.; Zhang, J. Z.; Hyeon, T. *J. Am. Chem. Soc.* **2003**, *125*, 11100–11105.

(3) (a) Bruchez, M., Jr.; Moronne, M.; Gin, P.; Weiss, S.; Alivisatos, A. P. *Science* **1998**, *281*, 2013–2016. (b) Gao, X.; Cui, Y.; Levenson, R. M.; Chung, L. W. K.; Nie, S. *Nat. Biotechnol.* **2004**, *22*, 969–976. (c) Wood, V.; Halpert, J. E.; Panzer, M. J.; Bawendi, M. G.; Bulovic, V. *Nano Lett.* **2009**, *9*, 2367–2371. (d) Brown, P.; Kamat, P. V. *J. Am. Chem. Soc.* **2008**, *130*, 8890–8891.

(4) (a) Zhong, X.; Feng, Y.; Knoll, W.; Han, M. *J. Am .Chem. Soc.* **2003**, *125*, 13559–13563. (b) Zhong, X.; Han, M.; Dong, Z.; White, T. J.; Knoll, W. *J. Am. Chem. Soc.* **2003**, *125*, 8589–8594.

(5) (a) Norris, D. J.; Yao, N.; Charnock, F. T.; Kennedy, T. A. *Nano Lett.* **2001**, *1*, 3–7. (b) Yang, Y.; Chen, O.; Angerhofer, A.; Cao, Y. C. *J. Am. Chem. Soc.* **2006**, *128*, 12428–12429. (c) Archer, P. I.; Santangelo, S. A.; Gamelin, D. R. *J. Am. Chem. Soc.* **2007**, *129*, 9808–9818. (d) Radovanovic, P. V.; Norberg, N. S.; McNally, K. E.; Gamelin, D. R. *J. Am. Chem. Soc.* **2002**, *124*, 15192–15193. (e) Nag, A.; Sapra, S.; Nagamani, C.; Sharma, A.; Pradhan, N.; Bhat, S. V.; Sarma, D. D. *Chem. Mater.* **2007**, *19*, 3252–3259. (f) Acharya, S.; Sarma, D. D.; Jana, N. R.; Pradhan, N. *J. Phys. Chem. Lett.* **2010**, *1*, 485–488. (g) Jana, S.; Srivastava, B. B.; Acharya, S.; Santra, P. K.; Jana, N. R.; Sarma, D. D.; Pradhan, N. *Chem. Commun.* **2010**, *46*, 2853–2855. (h) Srivastava, B. B.; Jana, S.; Karan, N. S.; Paria, S.; Jana, N. R.; Sarma, D. D.; Pradhan. *J. Phys. Chem. Lett* **2010**, *1*, 1454–1458. (i) Karan, N. S.; Sarma, D. D.; Kadam, R. M.; Pradhan, N. *J. Phys. Chem. Lett.* **2010**, *1*, 2863–2866. (j) Nag, A.; Chakraborty, S.; Sarma, D. D. *J. Am. Chem. Soc.* **2008**, *130*, 10605–10611. (k) Nag, A.; Sarma, D. D. *J. Phys. Chem. C* **2007**, *111*, 13641–13644. (l) Yang, Y.; Jin, Y.; He, H.; Wang, Q.; Tu, Y.; Lu, H.; Ye, Z. *J. Am. Chem. Soc.* **2010**, *132*, 13381–13394.

(6) (a) Viswanatha, R.; Sarma, D. D. *Chem. Asian J.* **2009**, *4*, 904–909. (b) Wittenberg, J. S.; Merkle, M. G.; Alivisatos, A. P. *Phys. Rev. Lett.* **2009**, *103*, 125701/1–125701/4. (c) Tolbert, S. H.; Alivisatos, A. P. *Science* **1994**, *265*, 373–6. (d) Wickham, J. N.; Herhold, A. B.; Alivisatos, A. P. *Phys. Rev. Lett.* **2000**, *84*, 923–926.

(7) (a) Chen, D.; Viswanatha, R.; Ong, G. L.; Xie, R.; Balasubramaninan, M.; Peng, X. *J. Am. Chem. Soc.* **2009**, *131*, 9333–9339. (b) Dalpian, G. M.; Chelikowsky, J. R. *Phys. Rev. Lett.* **2006**, *96*, 226802/1–226802/4. (c) Norris, D. J.; Efros, A. L.; Erwin, S. C. *Science* **2008**, *319*, 1776–1779.

(8) Qadri, S. B.; Skelton, E. F.; Hsu, D.; Dinsmore, A. D.; Yang, J.; Gray, H. F.; Ratna, B. R. *Phys. Rev. B: Condens. Mater. Phys.* **1999**, *60*, 9191–9193.

(9) Xue, L. A.; Raj, R. *J. Mater. Sci. Lett.* **1990**, *9* (7), 818–19.

(10) Ma, C.; Moore, D.; Li, J.; Wang, Z. L. *Adv. Mater.* **2003**, *15* (3), 228–231.

(11) (a) Datta, A.; Panda, S. K.; Chaudhuri, S. *J. Solid State Chem.* **2008**, *181* (9), 2332–2337. (b) Kar, S.; Biswas, S.; Chaudhuri, S. *Synth. React. Inorg. Met.—Org., Nano-Met. Chem.* **2006**, *36* (2), 193–196. (c) Wang, F. H., Y.; Lim, C. S.; Lu, Y.; Wang, J.; Xue, J; Chen, H.; Zhang, C.; Hong, M; Liu, X. *Nature* **2010**, *463*, 1061–1065.

(12) Murakoshi, K.; Hosokawa, H.; Tanaka, N.; Saito, M.; Wada, Y.; Sakata, T.; Mori, H.; Yanagida, S. *Chem. Commun.* **1998**, *3*, 321–322.

(13) (a) Wang, Z.; Daemen, L. L.; Zhao, Y.; Zha, C. S.; Downs, R. T.; Wang, X.; Wang, Z. L.; Hemley, R. J. *Nat. Mater.* **2005**, *4* (12), 922–927. (b) Erwin, S. C.; Zu, L.; Haftel, M. I.; Efros, A. L.; Kennedy, T. A.; Norris, D. J. *Nature* **2005**, *436* (7047), 91–94.

(14) (a) Bhargava, R. N.; Gallagher, D.; Hong, X.; Nurmikko, A. *Phys. Rev. Lett.* **1994**, *72* (3), 416–19. (b) Pradhan, N.; Peng, X. *J. Am. Chem. Soc.* **2007**, *129* (11), 3339–3347. (c) Sapra, S.; Prakash, A.; Ghangrekar, A.; Periasamy, N.; Sarma, D. D. *J. Phys. Chem. B* **2005**, *109* (45), 1663–1668.

(15) Yang, Y.; Chen, O.; Angerhofer, A.; Cao, Y. C. *J. Am. Chem. Soc.* **2008**, *130* (46), 15649–15661.

(16) (a) Williams, V. A. *J. Mater. Sci.* **1972**, *7* (7), 807–12. (b) Birman, J. L. *Phys. Rev.* **1959**, *115*, 1493–1505.

(17) Hamad, S.; Cristol, S.; Catlow, C. R. A. *J. Phys. Chem. B* **2002**, *106* (42), 11002–11008.